**Maltidis, Georgios; Stempniewski, Lothar**

# Fluid Structure Interaction Arch Dam - Reservoir at Seismic Loading

# Fluid Structure Interaction
## Arch Dam – Reservoir at Seismic Loading

**G. Maltidis[1], L. Stempniewski[2]**

[1] Federal Waterways Engineering and Research Institute, Kußmaulstrasse 17, 76187 Karlsruhe, GERMANY

[2] Karlsruhe Institute for Technology, Institute of Concrete Structures and Building Materials, Department of Concrete Structures, Gotthard-Franz-Str. 3, 76131, Karlsruhe, GERMANY

E-mail: georgios.maltidis@baw.de

## Abstract

The fluid structure interaction is an important issue that must be taken into account for the analysis and design of hydraulic structures. Since the first attempts to calculate the hydrodynamic pressures on structures analytically (Westergaard, von Kármán, Mononobe, Housner, Chwang, Zangar) the engineers and researchers have the last years a very useful tool, the finite and boundary element method, in order to analyze complicated structures taking into account different sophisticated phenomena. However, even nowadays, the common praxis is to use the early developed techniques, because of their simplicity and capability of implementation in the most finite element codes.

## Introduction

Since 1933, the hydrodynamic pressures on oscillating structures, which are in contact with water, are taken into account with the simplified assumption that the water is incompressible and the structure is star using the added mass approaches, first proposed by Westergaard for vertical star surfaces and later extended by Zangar for inclined surfaces. Although these approaches apply under conditions which hardly are met, they are widely used also nowadays because of their simplicity in incorporating them in finite element codes. However, the result of analysis with the added mass approach may come out to be very conservative leading to wrong decisions. The modeling of the water with finite solid element around the 1980's gave the opportunity for the analyst to take account some phenomena, as the water compressibility but raised other numerical problems as such type of modeling of water is suffering many times of hourglass making the analysis instable. The use of acoustic elements seems to be the more beneficial, as there are hardly numerical problems, and most of the phenomena, which take place for a dynamic fluid structure interaction can be modeled. With acoustic elements the analyst can consider the water compressibility, the wave absorption at the infinite end of the reservoir and the impedance of wave radiation at the reservoir sediments.

## Hydrodynamic Pressures

### Added mass approaches

The most well-known added mass approach is the one of Westergaard (1933)[1]. Westergaard proposed the following formula for the computation of hydrodynamic pressures as added masses under the restrictions that the reservoir is infinite, the upstream surface of the dam is vertical and the dam is rigid:

$$m = \frac{7}{8} \cdot \sqrt{H \cdot y} \cdot \frac{\gamma_w}{g} \cdot A \tag{1}$$

where m the added mass, H and y the height and the depth of the reservoir respectevily, $\gamma_w$ the density of the water, g the gravitational acceleration and A the contributing area around the node.

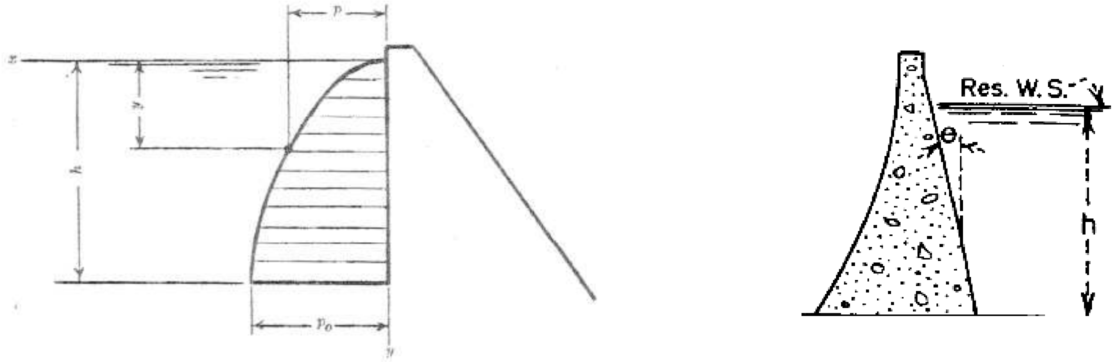


Figure 1: Graphical representation of Westergaard's and Zangar's calculation models.

Zangar (1952)[2], using an electric analogue, extended the added mass approach of Westergaard for inclined upstream surfaces of the dam, introducing reductive factors dependent on the angle of inclination.

$$m = 0,5 \cdot H \cdot C_m \cdot \left[ \frac{y}{H} \cdot (2 - \frac{y}{H}) + \sqrt{\frac{y}{H} \cdot (2 - \frac{y}{H})} \right] \cdot \frac{\gamma_w}{g} \cdot A \tag{2}$$

where $C_m$ a coefficient based on the angle of inclination and the other parameters as Westergaard's formula.

**Fluid Elements**

The fluid elements are solid elements to which the characteristics of the water are applied. The incompressibility or the water as well as the null shear resistance are introduced with a Poisson number equal with 0,5 or close to this value for the finite element programs. The bulk modulus of the water is K=2,2 GPa. The modeling of the water with solid elements causes numerical instabilities because of the introducing of zero energy modes (hourglass modes). This effect can be mitigated with the use of hourglass control and by applying the free surface boundary condition for the vertical node displacements [9]. Moreover, a nonlinear material behavior with tension cut off or a contact interaction which allows only compression to be transmitted will avoid unrealistic tension stress of the dam caused by the water.

**Acoustic Elements**

The acoustic elements are used to model the fluid behavior of the air. They have no shear and tension resistance and they transmit only pressures [10]. With assignment of the water bulk modulus they model the water behavior very good. Numerous boundary conditions can be assigned to the acoustic elements, which model natural phenomena such as wave absorption at the far end of the reservoir, sloshing of the free surface, wave impedance at the reservoir's bottom due to sediments etc. For the acoustic elements no special numerical care has to be taken except for assigning the boundary conditions.

**Model aspects**

For this benchmark two models (one with coarse mesh and one with fine mess) are investigated. The mesh of the reservoir is the same for both cases. The foundation was considered massless, so no further care was taken for wave absorption or deconvolution of the

seismic motion. Because of the massless foundation with no radiation absorption of the seismic waves and due to the lack of further non-linearities of the dam's material and of the contact interfaces, a big enough structural damping is applied. As presented in [6] for a big range of frequencies the total Rayleigh damping is between 8 and 10 %. Due to the linear finite element analysis a 10% viscous damping is used by [6]. Here, because of the small peak ground acceleration of 0,1g a value of 7,5% of structural damping was chosen in order to determine the Rayleigh stiffness damping factor a and the Rayleigh mass factor β.
For the reservoir hydrodynamic pressures, two added mass approaches and one reservoir modeling with acoustic elements were investigated. The generalized Westergaard's [11] and the Zangar's added mass approaches were used. The added masses were given via a user subroutine which defines user elements in Abaqus [5].
The two models with acoustic elements differ only in the wave absorption's method of the far field. The first uses acoustic infinite element whereas the latter impedance boundary condition. The impedance condition can be given either as element based or as surface based condition. Moreover a boundary condition is given at the reservoir free surface constraining the dynamic acoustic pressures to be zero. The surfaces of the rock and the dam are tied with the surfaces of the reservoir.

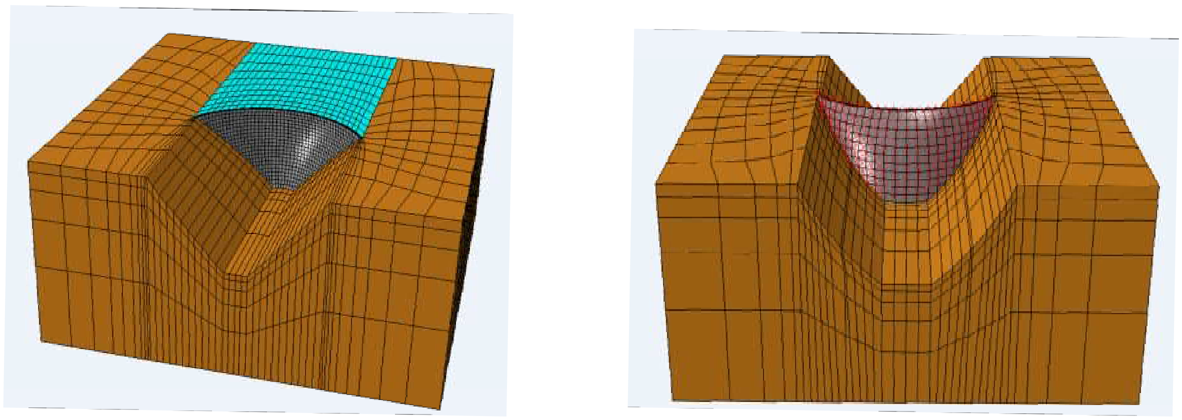

Figure 2: The model with two different meshes and two reservoir modeling approaches: left fine mesh and acoustic elements and right coarse mesh and added mass elements.

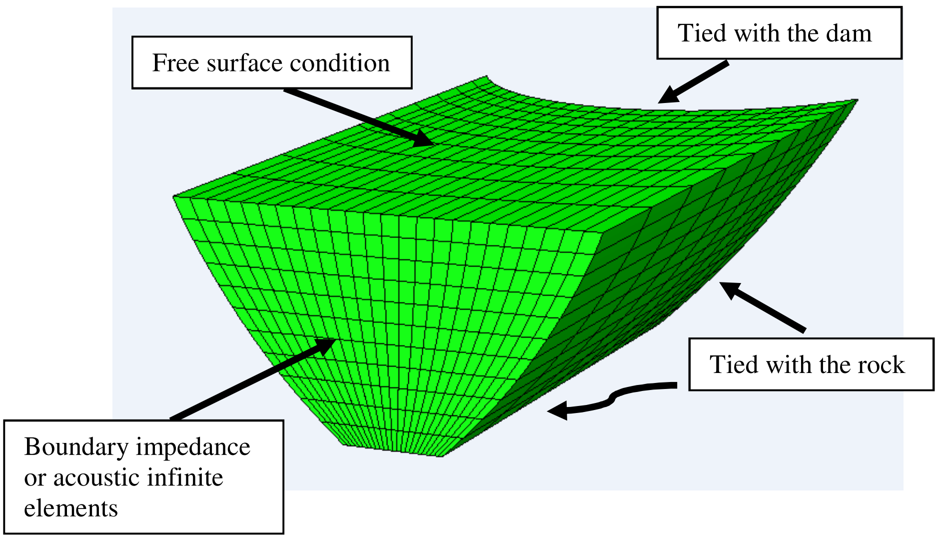


Figure 3: The reservoir with its boundary conditions.

Table 1: Material Parameters

| | Rock | Water | Dam |
|---|---|---|---|
| Density (kg) | 0 | 1000 | 2400 |
| Poisson Ratio | 0,2 | - | 0,167 |
| Young Modulus (MPa) | 25000 | - | 27000 |
| Bulk Modulus (MPa) | - | 2200 | - |

**Analysis' methods**

The seismic analyses were carried out using the time history with direct integration and the modal time history. From computational time the modal time history is a little bit faster than the time history with direct integration. The time histories were gives as nodal acceleration to the boundaries of the rock. A baseline correction offered by Abaqus was also applied to them.

**Results**

The results of the analyses are presented at the next tables and diagrams. The first table shows the ten first modes for the dam, with empty and with full reservoir modeled by the different methods described before. The diagrams show due to lack of space only some of the results containing the minimal and maximal vertical, minimum principal and maximum principal stresses of the dam for the different reservoir models and for the different dam mesh. The results are given for the paths along the height of the dam, for the upstream and the downstream sections. For convenience abbreviations were introduced to the diagrams (e.g. "*dti*" refers to direct time integration, "*West*" to Westergaard's added mass, "*ac*" to acoustic element, "*imp*" to impedance boundary condition for the acoustic elements, "*inf*" to acoustic infinite elements, "*modal*" to modal dynamic analysis). The results for the fine mesh model are given with dashpot line in order to differ easier than the ones of the coarse mesh model.

The analysis with the infinite elements had more computational cost than the analysis with the impedance condition. In order to obtain similar results to the impedance boundary condition with the use of infinite acoustic elements, care must be given in the definition of the infinite elements' thickness. There are trivial differences when the analyst uses the improved rather than the planar non-reflecting condition offered by Abaqus.

The results of the fine model with acoustic elements for the reservoir gave too conservative results. The author believes that these results for the given meshes of dam and reservoir are not correct due to violation of the contact condition, according to which the slave surface nodes must be finer than the master surface nodes.

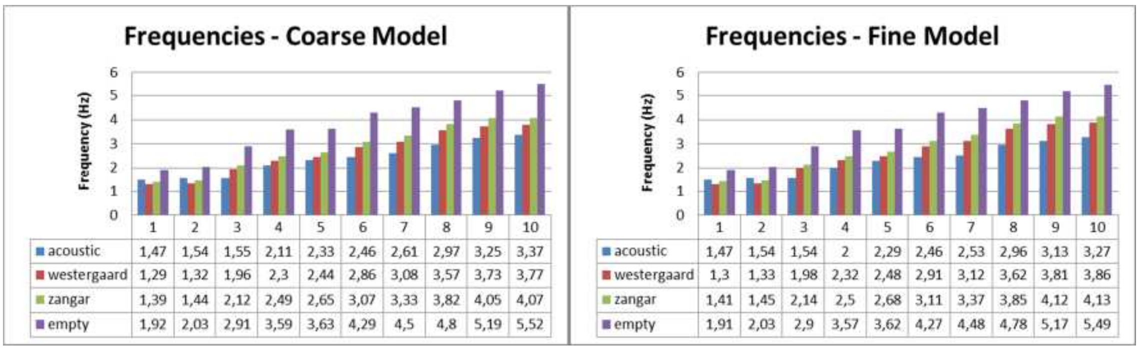


Figure 4: The frequencies for the two models (coarse left, fine right) and for the four reservoir models.

Table 2: Ten first modes for the coarse model

| Mode Nr. | Empty | | Acoustic | | Westergaard | | Zangar | |
|---|---|---|---|---|---|---|---|---|
| | f (Hz) | T (sec) | f (Hz) | T (sec) | f (Hz) | T (sec) | f (Hz) | T (sec) |
| 1 | 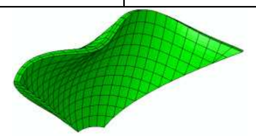 f=1,92 | T=0,52 | 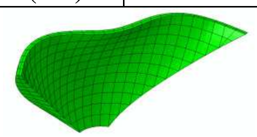 f=1,47 | T=0,68 | 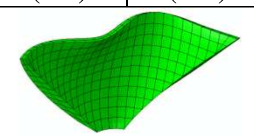 f=1,29 | T=0,78 | 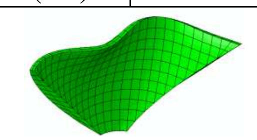 f=1,39 | T=0,72 |
| 2 | 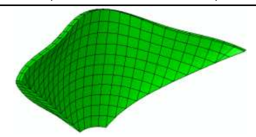 f=2,03 | T=0,49 | 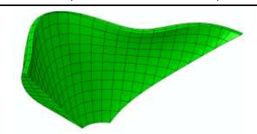 f=1,54 | T=0,65 | 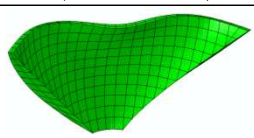 f=1,32 | T=0,76 | 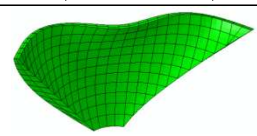 f=1,44 | T=0,69 |
| 3 | 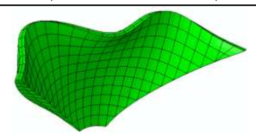 f=2,91 | T=0,34 | 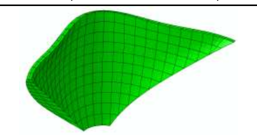 f=1,55 | T=0,65 | 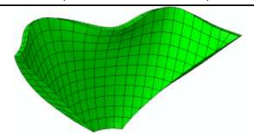 f=1,96 | T=0,51 | 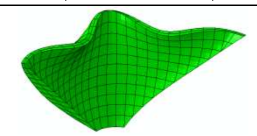 f=2,12 | T=0,47 |
| 4 | 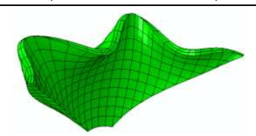 f=3,59 | T=0,28 | 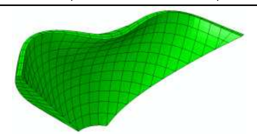 f=2,11 | T=0,47 | 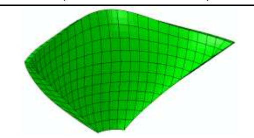 f=2,30 | T=0,43 | 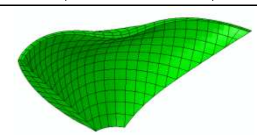 f=2,49 | T=0,40 |
| 5 | 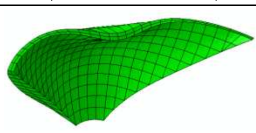 f=3,63 | T=0,28 | 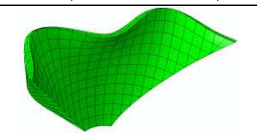 f=2,33 | T=0,43 | 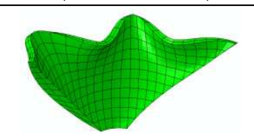 f=2,44 | T=0,41 | 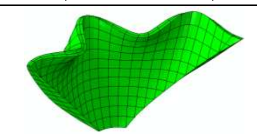 f=2,65 | T=0,38 |
| 6 | 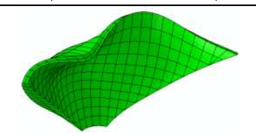 f=4,29 | T=0,23 | 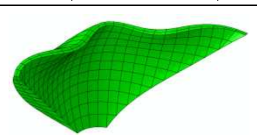 f=2,46 | T=0,41 | 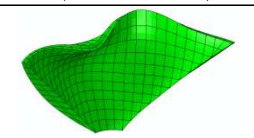 f=2,86 | T=0,35 | 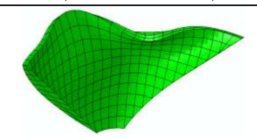 f=3,07 | T=0,33 |
| 7 | 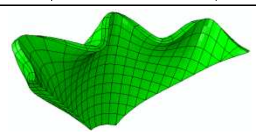 f=4,50 | T=0,22 | 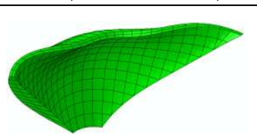 f=2,61 | T=0,38 | 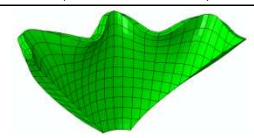 f=3,08 | T=0,32 | 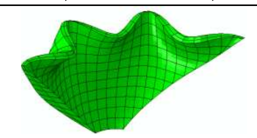 f=3,33 | T=0,30 |
| 8 | 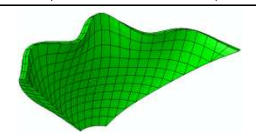 f=4,80 | T=0,21 | 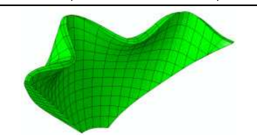 f=2,97 | T=0,34 | 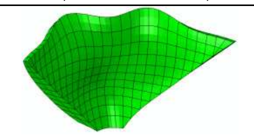 f=3,57 | T=0,28 | 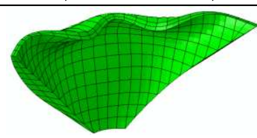 f=3,82 | T=0,26 |
| 9 | 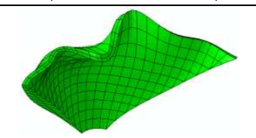 f=5,19 | T=0,19 | 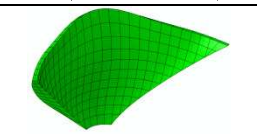 f=3,25 | T=0,31 | 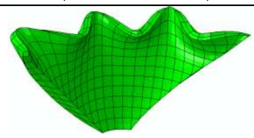 f=3,73 | T=0,27 | 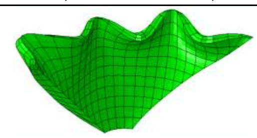 f=4,05 | T=0,25 |
| 10 | 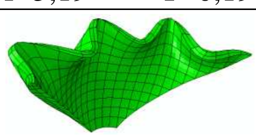 f=5,52 | T=0,18 | 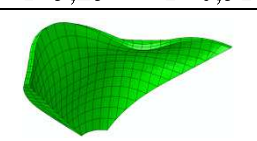 f=3,37 | T=0,30 | 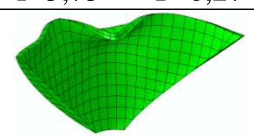 f=3,77 | T=0,27 | 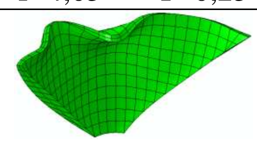 f=4,07 | T=0,25 |

Table 3: Ten first modes for the fine model

| Mode Nr. | Empty | | Acoustic | | Westergaard | | Zangar | |
|---|---|---|---|---|---|---|---|---|
| | f (Hz) | T (sec) | f (Hz) | T (sec) | f (Hz) | T (sec) | f (Hz) | T (sec) |
| 1 | 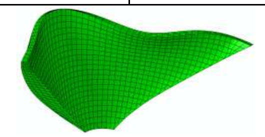 f=1,91 | T=0,52 | 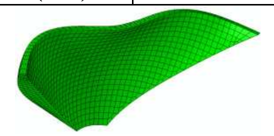 f=1,47 | T=0,68 | 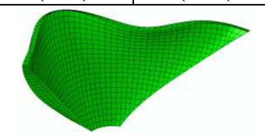 f=1,30 | T=0,77 | 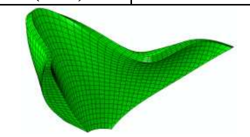 f=1,41 | T=0,71 |
| 2 | 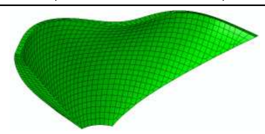 f=2,03 | T=0,49 | 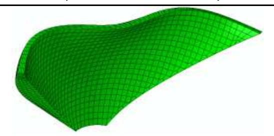 f=1,54 | T=0,65 | 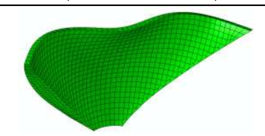 f=1,33 | T=0,75 | 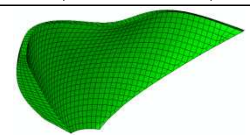 f=1,45 | T=0,69 |
| 3 | 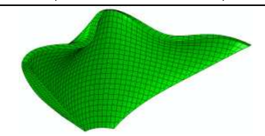 f=2,90 | T=0,35 | 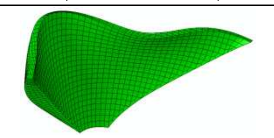 f=1,54 | T=0,65 | 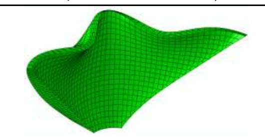 f=1,98 | T=0,50 | 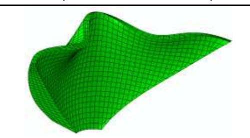 f=2,14 | T=0,47 |
| 4 | 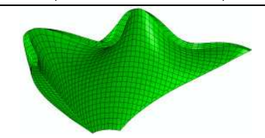 f=3,57 | T=0,28 | 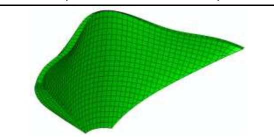 f=2,00 | T=0,50 | 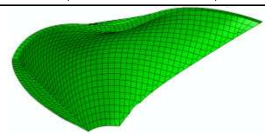 f=2,32 | T=0,43 | 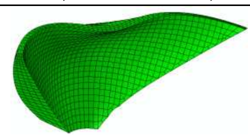 f=2,50 | T=0,40 |
| 5 | 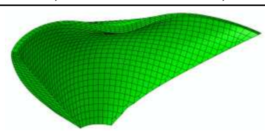 f=3,62 | T=0,28 | 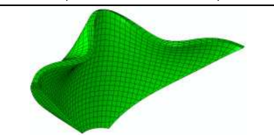 f=2,29 | T=0,44 | 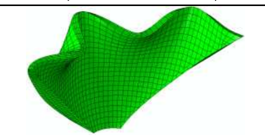 f=2,48 | T=0,40 | 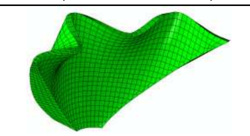 f=2,68 | T=0,37 |
| 6 | 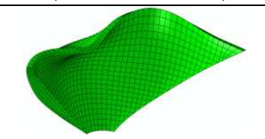 f=4,27 | T=0,23 | 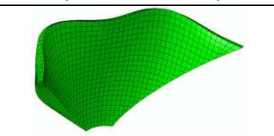 f=2,46 | T=0,41 | 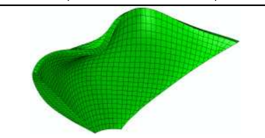 f=2,91 | T=0,34 | 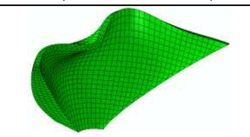 f=3,11 | T=0,32 |
| 7 | 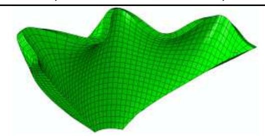 f=4,48 | T=0,22 | 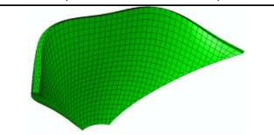 f=2,53 | T=0,40 | 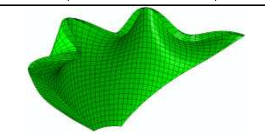 f=3,12 | T=0,32 | 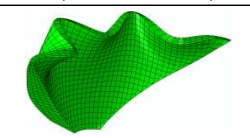 f=3,37 | T=0,30 |
| 8 | 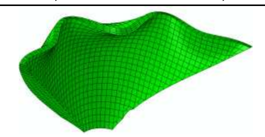 4,78 | T=0,21 | 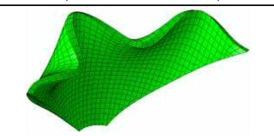 f=2,96 | T=0,34 | 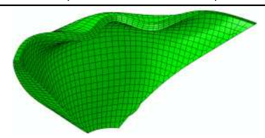 f=3,62 | T=0,28 | 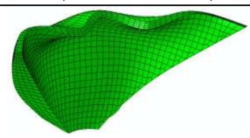 f=3,85 | T=0,26 |
| 9 | 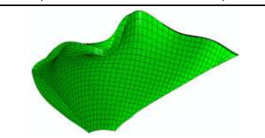 f=5,17 | T=0,19 | 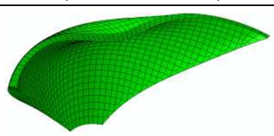 f=3,13 | T=0,32 | 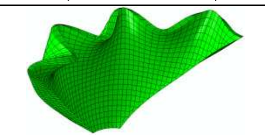 f=3,81 | T=0,26 | 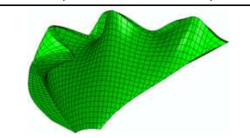 f=4,12 | T=0,24 |
| 10 | 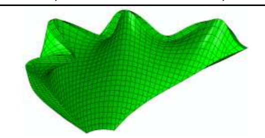 f=5,49 | T=0,18 | 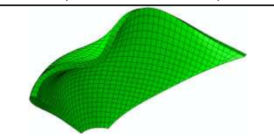 f=3,27 | T=0,31 | 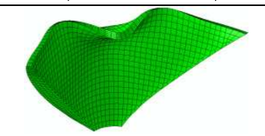 f=3,86 | T=0,26 | 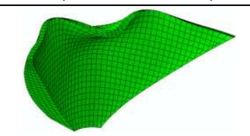 f=4,13 | T=0,24 |

The next diagrams give some representative comparisons between results for the different reservoir models and analysis' methods.

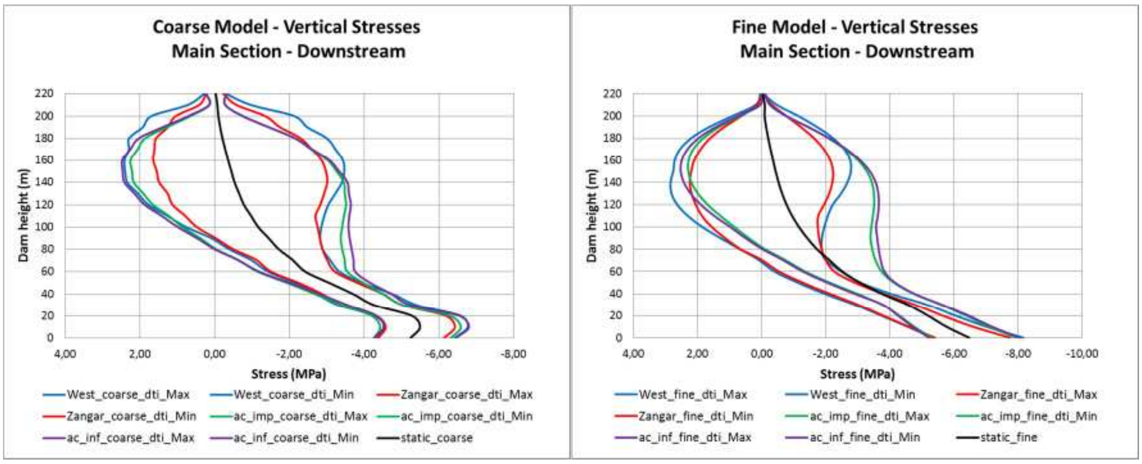


Figure 6: The vertical stresses for the different reservoir models at the downstream main section.

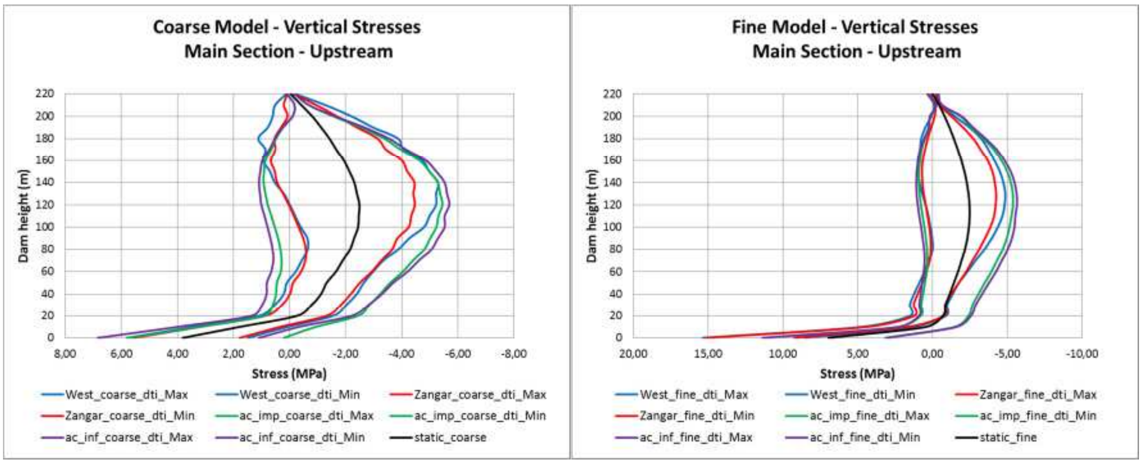


Figure 7: The vertical stresses for the different reservoir models at the upstream main section.

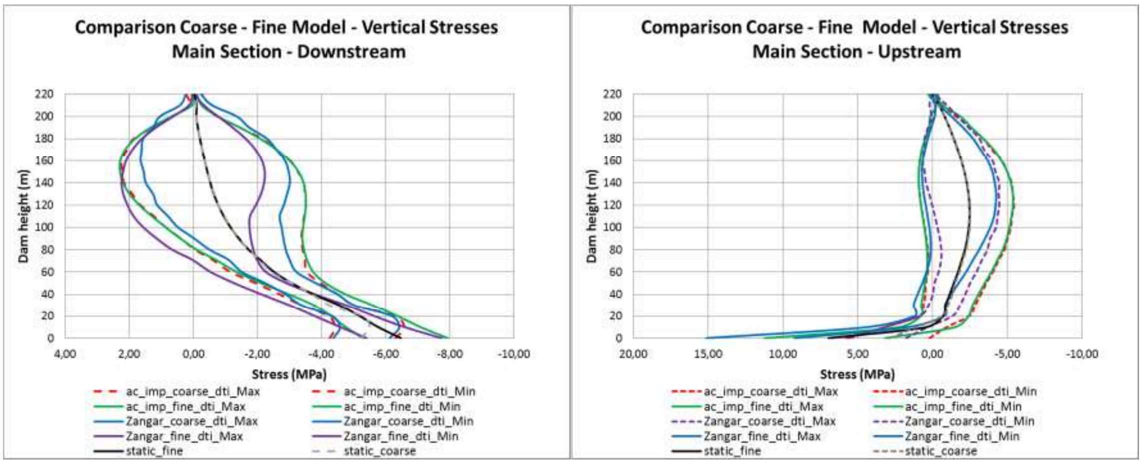


Figure 8: Comparison between the coarse and fine model for the vertical stresses.

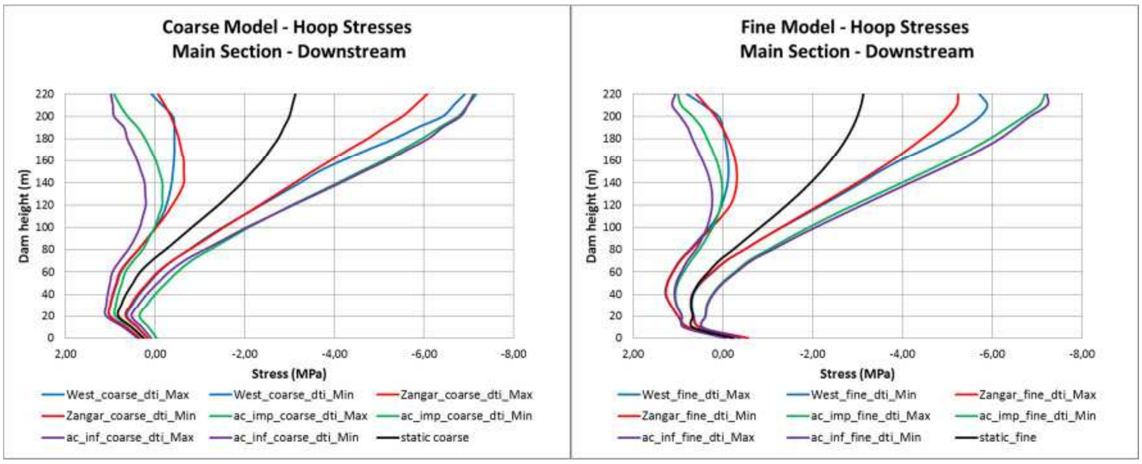


Figure 9: The hoop stresses for the different reservoir models at the downstream main section.

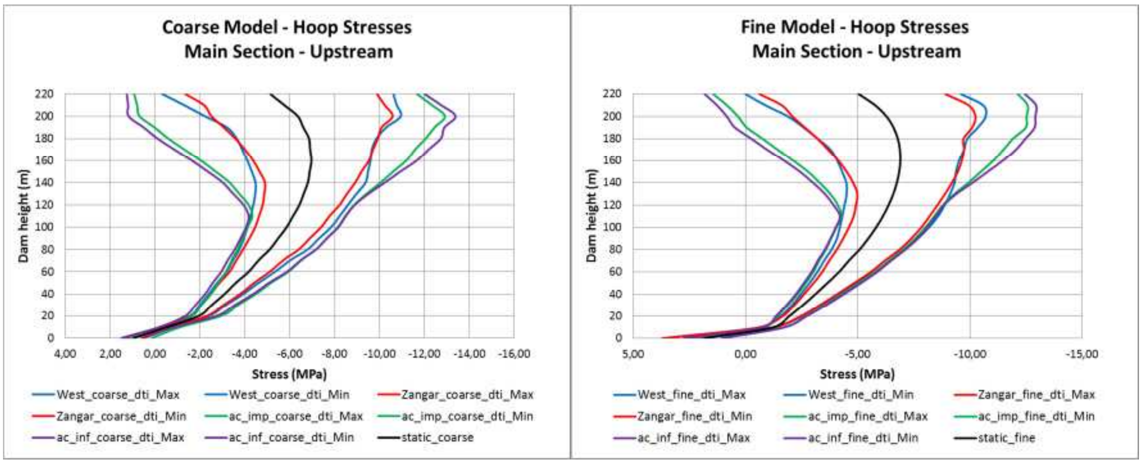


Figure 10: The hoop stresses for the different reservoir models at the upstream main section.

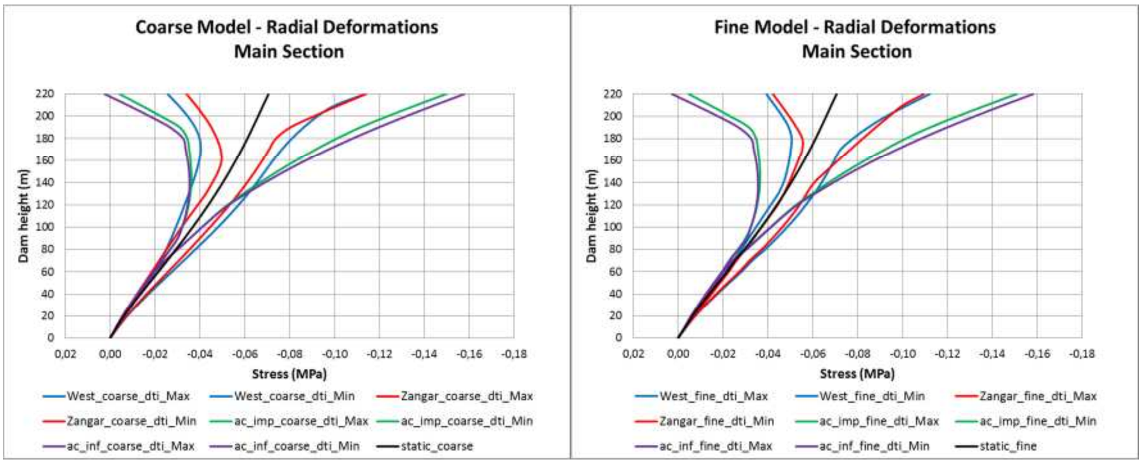


Figure 11: The radial deformations for the different reservoir models at the main section.

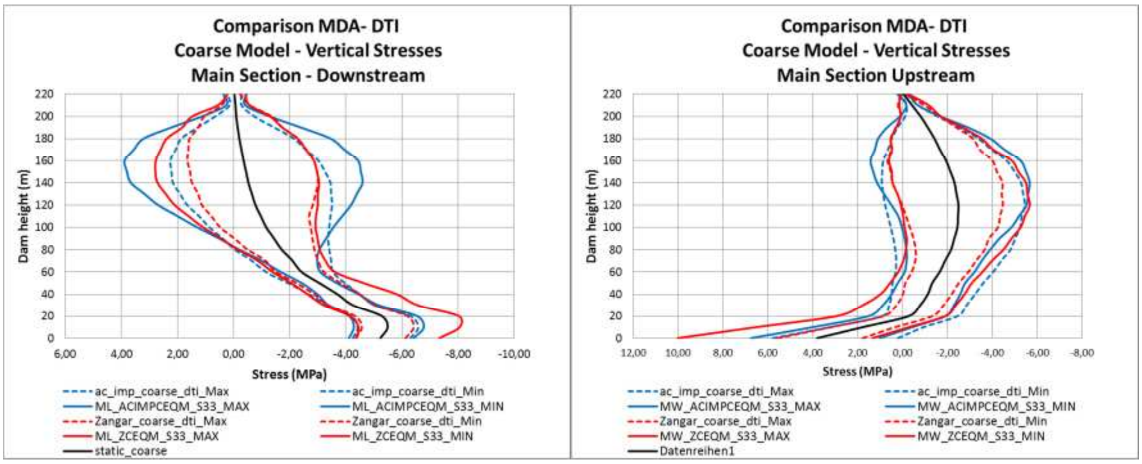


Figure 12: Comparison between the modal dynamic analysis and the direct time integration for the coarse model with the Zangar's approach at the downstream (left) and upstream (right) main section.

# Conclusion

The earthquake analysis of an arch dam-reservoir-foundation system was performed with different modeling aspects according to the formulators' directions. The results show very near values for the two added mass approaches, with the one of Zangar to be a little bit more favorable than the one of Westergaard. The acoustic elements models with the two non-reflecting approaches give identical results. The coarse and fine models differ only in the base stresses due to the coarser mess of the coarse model and some deviations are noticed at the added mass models. Although the modal dynamic analysis is much faster than the direct time integration, delivers conservative results.

# Acknowledgements

This paper consists a part of the research project „Earthquake Analysis and Design of Hydraulic Structures", which is funded by the Federal Waterways and Research Institute of Germany in cooperation with the Institute of Concrete Structures of the Karlsruhe Institute for Technology. The contribution of both participated Institutes and persons involved is highly acknowledged.

# References

[1] Westergaard, H. M. (1933). Water pressures on dams during earthquakes. Transactions of the American Society of Civil Engineers, American Society of Civil Engineers, New York, New York, Paper 1835, 1933.

[2] Zangar, C. N. (1952). Hydrodynamic Pressures on dams due to horizontal earthquake effects. U.S. Departmant of Interior, Bureaus of Reclamation, Engineering Monographs No.11

[3] Chwang, A.T., Housner, G.W. (1978). Hydrodynamic pressures on sloping dams during earthquakes. Part 1. Momentum Method. Journal of Fluid Mechanics, vol. 2, part 2, pp. 335-341

[4] Chwang, A.T. (1978). Hydrodynamic pressures on sloping dams during earthquakes. Part 2. Exact Theory. Journal of Fluid Mechanics, vol. 2, part 2, pp. 343-348

[5] ABAQUS (2011),*User's manual, Version 6.11*. Dassault Systèmes Simulia Corporation, Providence RI, USA.
[6] US Bureau of Reclamation (2006), State-of-Practice for the NonlinearAnalysis of Concrete Dams at the Bureau of Reclamation, USBR Report, Colorado, USA.
[7] United States Society on Dams (2008). Numerical models for seismic evaluation of concrete dams. Review, evaluation and interpretation of results. USSD, Denver, USA.
[8] Zienkiewicz, O. C., Bettess, P. (1978). Fluid-Structure dynamic interaction and wave forces. An introduction to numerical treatment. International Journal For Numerical Methods In Engineering, Vol. 13, 1-16.
[9] Wilson, E.D., Khalvati,M. (1983). Finite elements for the dynamic analysis of fluid-solid systems. International Journal For Numerical Methods In Engineering, Vol. 19, 1657-1668.
[10] Matthew Muto, Nicolas von Gersdorff, Zee Duron, Mike Knarr (2012). *Effective Modeling of Dam-Reservoir Interaction Effects Using Acoustic Finite Elements*, in Proceedings of Innovative Dam and Levee Design and Construction for Sustainable Water Management, 32nd Annual USSD Conference, New Orleans, Louisiana, April 23-27, 2012, Pages 1161-1168.
[11] Kuo, James Shaw-Han, (1982). Fluid-structure interactions: added mass computations for incompressible fluid. UCB/EERC-82/09, Earthquake Engineering Research Center, University of California, Berkeley, 1982-08.